

InSpaceType: Dataset and Benchmark for Reconsidering Cross-Space Type Performance in Indoor Monocular Depth

Cho-Ying Wu¹
choyingw@usc.edu

Quankai Gao¹
quankaig@usc.edu

Chin-Cheng Hsu¹
chincheh@usc.edu

Te-Lin Wu²
telinwu@g.ucla.edu

Jing-Wen Chen¹
jchen885@usc.edu

Ulrich Neumann¹
uneumann@usc.edu

¹ Computer Science Department
University of Southern California
California, USA

² Computer Science Department
University of California, Los Angeles
California, USA

Abstract

Indoor monocular depth estimation helps home automation, including robot navigation or AR/VR for surrounding perception. Most previous methods primarily experiment with the NYUv2 Dataset and concentrate on the overall performance in their evaluation. However, their robustness and generalization to diversely unseen types or categories for indoor spaces (spaces types) have yet to be discovered. Researchers may empirically find degraded performance in a released pretrained model on custom data or less-frequent types. This paper studies the common but easily overlooked factor- space type and realizes a model's performance variances across spaces. We present InSpaceType Dataset, a high-quality RGBD dataset for general indoor scenes, and benchmark 13 recent state-of-the-art methods on InSpaceType. Our examination shows that most of them suffer from performance imbalance between head and tailed types, and some top methods are even more severe. The work reveals and analyzes underlying bias in detail for transparency and robustness. We extend the analysis to a total of 4 datasets and discuss the best practice in synthetic data curation for training indoor monocular depth. Further, dataset ablation is conducted to find out the key factor in generalization. This work marks the first in-depth investigation of performance variances across space types and, more importantly, releases useful tools, including datasets and codes, to closely examine your pretrained depth models. Data and code: <https://depthcomputation.github.io/DepthPublic/>

1 INTRODUCTION

Depth estimation from monocular images is long-studied [8, 9, 8, 14, 15, 17, 23, 24, 25, 26, 34, 37, 45, 50, 50, 52] and widely used in industry for indoor automation nowadays,

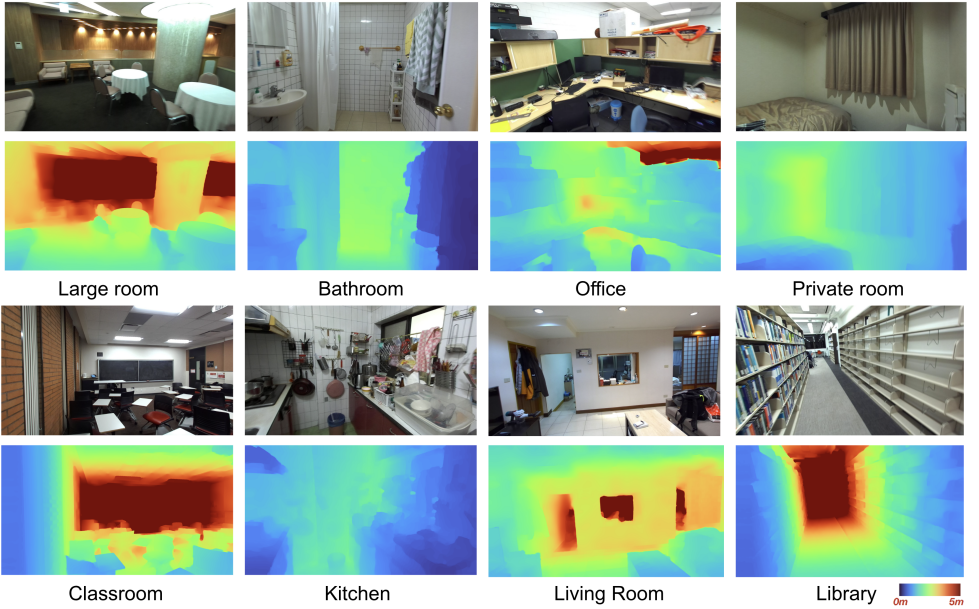


Figure 1: **InSpaceType** data samples. We color depth within 5 meters to show the near field. The captured data are dense, high-quality, and high-resolution for modern applications.

such as collision detection [13] and navigation [44] for home robots, surrounding sensing in AR/VR [11, 22, 30], and RGBD approaches for biometrics surveillance [20]. It also helps learn better 3D representations in neural fields [10].

Either recent works of using large models and training on multiple datasets such as ZoeDepth [2], DepthAnything [49], and Unidepth [32], or prior methods of single-dataset train/ test [3, 6, 6, 12, 17, 21, 23, 24, 28, 52] primarily focus on the NYUv2 dataset [40] for benchmark and evaluation. Though showing top performance on the benchmark, researchers may empirically find degraded performance on custom data or observe irregular depth prediction from unseen textures or spaces that rarely appear in those models’ training sets, such as oriental-style rooms. Robustness for real-world usage is not guaranteed.

We spot common shortcomings for the popular NYUv2 evaluation and benchmark: (1) Evaluation always reports metrics on the whole test set and overlooks the *performance variances* across different space types¹. A model may perform better in types appearing more often (head type) than those less-frequent types (tailed type). (2) NYUv2 is limited by a decade-old Kinect-v1 sensor that suffers from relatively low resolution (480×640), noisy and blurry imaging, and limited measurable ranges. These downsides make the evaluation less reliable for modern robotics and high-resolution depth in AR/VR displays. Most prior depth estimation focuses on methodology and puts less focus on data and evaluation. However, as the monocular depth research matures, it is essential to investigate whether these models are ready for real usage with rigorous quality assessment.

We present a novel dataset, **InSpaceType**, to overcome the limitations and fulfill our study on performance variances across spaces. It is collected by a recent high-quality and

¹Space type in this work is defined by a space’s function, such as bedroom, kitchen, or library. Some open-plan rooms, like condos, are included in the data, and we classify their types by the function of each captured scene

high-resolution stereo camera with much better sensor characteristics than Kinect-v1.

Space type-focused. InSpaceType defines a hierarchical graph where each node is a type, and there are 26 leaf-node types in total that are representative and commonly seen in the real world. See the supplementary for the full graph. 13 recent high-performing methods with their pretrained models are used to benchmark the zero-shot performance for overall results and detailed space type breakdowns. Results show that imbalance exists in most methods, which are biased towards head types such as private room (MIM [48]’s $\delta_1=94.54$) and against tailed types such as large room (MIM’s $\delta_1=54.93$).

Beyond NYUv2. In addition to NYUv2, three other popular training sets are examined, including SimSIN [46], UniSIN [46], and Hypersim [58]. We show space type breakdowns for models trained on them and reveal underlying bias to specify proper usage of them for future research. In particular, we find synthetic datasets fail to reflect the real-scene complexity of cluttered and small objects, where models trained on synthetic datasets tend to underperform.

This work emphasizes the importance of the usually overlooked factor- *space type*. In addition to analysis in the paper, we provide a quality assessment tool, including datasets and codes that show hierarchical type reports, to closely analyze your pretrained model.

2 Related Work

2.1 Methods for Indoor Monocular Depth

Several methods leverage paired image and groundtruth depth from indoor RGBD sensors to train depth estimation models. Many high-performing methods are transformer-based including NeWCRFs [52], DepthFormer [23], PixelFormer [0], GLPDepth [17], MIM [48], AiP-T [60]. Some explore planarity or normal, including BTS [19] and IronDepth [8]. Some train on multiple datasets of indoor, outdoor, or unbounded scenes, including MiDaS [35], LeReS [51], DPT [66], ZoeDepth [0], VPD [54], DepthAnything [49], and Unidepth [32]. These models learn generic image-to-depth mappings, but to estimate metric depth on a specific domain, most of them need a fine-tune set, usually NYUv2 for indoor scenes. Uniquely, Unidepth shows strong generalizability that does not need a fine-tune set and still slightly wins over DepthAnything on NYUv2. There are few self-supervised methods that predict depth with physical indoor scales. For example, DistDepth [46] trains on simulated indoor stereo with left-right consistency, and GasMono [53] refines poses to recover scales.

Most of the above methods evaluate indoor performance only on NYUv2, and all of them only report overall performance, while performance variation across spaces is important for in-the-wild robustness. This work pioneers the evaluation by space types. We show detailed prediction variances with transparency in robustness for these methods. Later results show that most top-performing methods still suffer from imbalances between head and tailed types, and even for some top methods, the gaps are prominent.

2.2 Evaluation Protocol for Indoor Monocular Depth

Diode [44] collects both outdoor and indoor scenes with high-quality data but very low diversity of 2 scenes for evaluation only. IBims-1 [18] is limited to only 20 test scenes and 100 RGBD pairs. VA [46] renders photo-realistic synthetic images but is limited to only one scene. NYUv2 [40] is prevalent in indoor monocular depth and contains 654 RGBD

test pairs. However, NYUv2 was collected by a decade-old device, Kinect-v1. First, its accurate and measurable ranges are only up to 3.5m from the hardware analysis [14], and farther measurements are highly noisy since the laser power dissipates quadratically with distance. Further, the sensor captures incomplete depth where lasers were absorbed, renders high imaging noise and blur by an older camera ISP, and outputs low-resolution RGBD data with only VGA size (640×480). Compared with modern devices, NYUv2 is outdated in meeting the current application needs for robotics or high-resolution depth for AR/VR displays. NYUv2 contains small private rooms as the majority, and the benchmark only reports overall performance, which is thus dominated by the head type performance.

To overcome the limitations, we adopt a recently released high-quality stereo camera system, ZED-2i, to collect images and depth. From the sensor specification, ZED-2i estimates $< 1\%$ error for up to 3m depth and $< 5\%$ error for up to 15m depth. To verify, we use Kinect-v1 and ZED-2i to measure objects placed at 3m, 8m, and 15m. At 3m, both sensors predict about 0.8% error. At 8m, ZED-2i's error is about 2.7%, and Kinect's is about 10.8%. At 15m, ZED-2i gets about 4.2% error, but Kinect does not receive laser returns. Compared with Kinect, ZED-2i gets denser depth, much higher depth resolution (2208×1242), and cleaner and sharper RGB imaging quality by a recent camera ISP. Our collected InSpaceType covers general-purpose and highly diverse 88 indoor scenes, including private household spaces, workspace, campus scenes, and other functional spaces, amounting to 1260 RGBD pairs. Our tool diagnoses a given model that shows the error and accuracy of each space type.

3 InSpaceType Dataset

Device and Data Capture. The adopted stereo camera, Zed-2i, has a baseline of 12cm, a field of view (FOV) of 120° , a maximally measurable distance of 20m, and optimized dense depth maps by its on-device model with errors verified in Sec. 2.2. Its setting gets 2208×1242 resolution at 15 fps for aligned images and depth. The device is anchored on a hand-held stabilizer for data capture. Our environments cover household spaces, workspace, campus, and functional spaces with 26 leaf node types. 88 different environments are visited in total. Non-Lambertian surfaces (mirrors or highly reflective areas) are avoided. We run at the full 120° FOV and do not crop, zoom-in, or focus at flat walls that reduce cues for scene depth. The camera moves at 6DoF with rotation and translation during capture. For the Euler rotation angles, yaw is unconstrained with $\pm 180^\circ$, where large yaw panning makes nearby frames less overlapped, pitch is within about $\pm 30^\circ$, and roll is within $\pm 10^\circ$. The constraints avoid reduced depth cues by larger pitch and roll, such as looking straight up to the ceiling.

Evaluation set. We manually select 1260 images from all the environments to create the evaluation set. Our selection criteria include (1) minimal motion blur, (2) not selecting from nearby 8 frames, and (3) sufficient depth cues (no single planes or zoom-in views) in the scenes. Fig. 1 shows sample images, and Fig. 2 shows the dataset statistics. Note that each type is not evenly distributed, which reflects the natural distribution, such as libraries appearing less frequent than private rooms. We do not favor or downsample common types to balance with the uncommon ones. To explain first, the distribution affects overall performance in Sec. 4-I, *whose purpose is to know how a model performs naturally and does not favor uncommon types*. Space type breakdowns and analysis in Sec. 4-II and III cancel the uneven distribution by averaging all samples in a type for evaluation metrics. *It leaves out the factor of number of samples in a type* and compares them against the other types to reveal a model's strength and weakness.

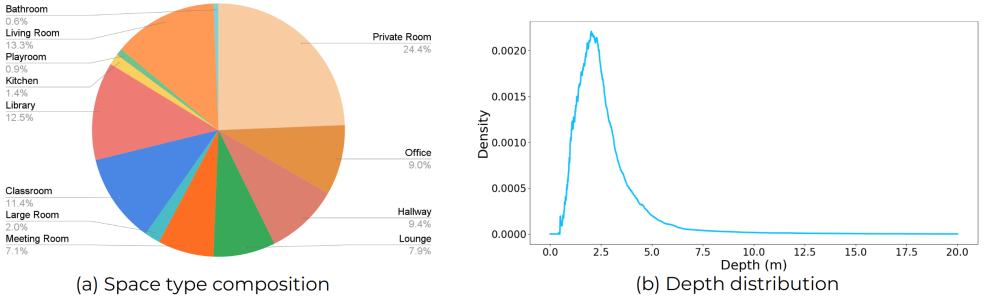


Figure 2: **Statistics of InSpaceType Evaluation Set.** Note that the type percentage affects the overall results in Table 1 but does not affect space type breakdowns in Table 2 and 3, as each type performance is computed by *averaging across all samples in a type* and compared to other types.

Table 1: **InSpaceType benchmark: overall performance.** The best number is in bold, and the second-best is underlined. We include 13 recent high-performing methods.

Method	Year	Architecture	AbsRel	SqRel	RMSE	δ_1	δ_2	δ_3
BTS [46]	arXiv'19	DenseNet-161	0.1445	0.1162	0.5222	81.65	95.57	98.54
AdaBins [8]	CVPR'21	Unet+AdaBins	0.1333	0.0957	0.4922	83.64	96.36	98.92
DPT [47]	ICCV'21	DPT-Hybrid	0.1224	0.0773	0.4616	85.96	97.17	99.19
GLPDepth [48]	arXiv'22	Mit-b4	0.1239	0.0788	0.4527	86.05	97.36	99.16
IronDepth [9]	BMVC'22	EfficientNet-B5	0.1276	0.1022	0.4894	85.30	96.37	98.84
Decomposition [49]	ECCV'22	EfficientNet-B5	0.1278	0.1025	0.4899	85.25	96.35	98.83
NeWCRFs [50]	CVPR'22	Swin-L	0.1251	0.0823	0.4541	86.04	96.68	98.94
PixelFormer [10]	WACV'23	Swin-L	0.1225	0.0761	0.4392	86.08	97.03	99.10
MIM [51]	CVPR'23	SwinV2-L	0.1100	0.0679	0.4244	88.58	97.59	99.28
VPD [52]	ICCV'23	StableDiffusion	0.0983	0.0661	0.4138	90.23	97.48	99.22
ZoeDepth (NK) [11]	arXiv'23	BeiT-L	0.0969	0.0527	0.3834	90.76	98.19	99.50
ZoeDepth (N) [11]	arXiv'23	BeiT-L	0.0956	0.0528	0.3887	<u>90.81</u>	<u>98.22</u>	99.52
DepthAnything [49]	CVPR'24	ViT-L	<u>0.0928</u>	<u>0.0506</u>	<u>0.3806</u>	90.01	98.09	<u>99.54</u>
UniDepth [53]	CVPR'24	ViT-L	0.0718	0.0349	0.3132	94.76	98.75	99.62

4 Benchmarks on InSpaceType

[I: Overall performance] The analysis aims to understand how a method performs naturally. We benchmark zero-shot cross-dataset performance on InSpaceType for 13 recent high-performing methods using their released indoor depth models, including DPT [47], GLPDepth [48], AdaBins [8], PixelFormer [10], NeWCRFs [50], BTS [46], MIM [51], IronDepth [9], Decomposition [49], VPD [52], ZoeDepth [11], DepthAnything [49], and Unidepth [53]. We adopt error (AbsRel, SqRel, RMSE; the lower, the better) and accuracy metrics (δ_1 , δ_2 , δ_3 with a base factor of 1.25; the higher, the better) commonly used in monocular depth estimation. To compensate for different camera intrinsics between their training set and InSpaceType, we follow prior protocols for cross-dataset evaluation [49, 54]: use median-scaling to align prediction and groundtruth's scales first and then calculate the metrics.

Analysis. Table 1 shows the comparison for overall performance. VPD, MIM, ZoeDepth, DepthAnything, and Unidepth are among the top-performing methods. They commonly adopt transformers [9, 10, 55] and learn better representations by large models. VPD learns from Stable Diffusion [56] and utilizes its pretrained image priors to help learn geometry. ZoeDepth and DepthAnything are first pretrained on a mixture of datasets, including indoor and outdoor scenes, and then fine-tuned on NYUv2 for the benchmark. In contrast, Unidepth does not require fine-tuning, and its paper reports zero-shot performance on NYUv2 that

Table 2: Space type breakdowns. In each block of the table, we show a performance breakdown and an easy/hard type summary (See Sec.4-II). The first N-only block includes top methods, MIM and PixelFormer, for training on RGBD data only from NYUv2. The M&LS-Pre blocks show four top methods, ZoeDepth, VPD, DepthAnything, and Unidepth, for those pretrained on multiple datasets or using large-scale pretraining with/without fine-tuning. We highlight the best and worst scores of each metrics. For standard deviation in each block, where methods are in the same category and around the same publishing time, we show the lowest values in boldface, indicating low imbalance, and the second one with underlines.

◊ N-only		MIM Results						PixelFormer Results					
Type Breakdown	AbsRel	SqRel	RMSE	δ_1	δ_2	δ_3		AbsRel	SqRel	RMSE	δ_1	δ_2	δ_3
Private room	0.0927	0.0342	0.2556	92.05	98.99	99.83		0.1013	<u>0.0372</u>	0.2638	90.17	98.70	99.80
Office	0.1106	0.0532	0.3313	87.67	97.42	99.44		0.1271	0.0649	0.3658	84.60	96.38	99.19
Hallway	0.1229	0.0805	0.5463	85.66	96.52	98.89		0.1418	0.0880	0.5236	81.46	96.40	99.05
Lounge	0.1316	0.1290	0.7447	84.15	96.22	98.93		0.1500	0.1624	0.8215	79.92	94.79	98.41
Meeting room	0.0984	0.0483	0.3636	91.70	98.69	99.64		0.1103	0.0551	0.3873	88.25	98.57	99.76
Large room	0.2683	0.4499	1.3915	54.93	83.89	93.91		0.2125	0.3119	1.1396	67.71	88.59	95.40
Classroom	0.0781	0.0334	0.3071	94.52	<u>99.25</u>	<u>99.83</u>		0.0912	0.0403	0.3368	91.37	<u>99.14</u>	<u>99.86</u>
Library	0.1342	0.0978	0.6281	85.61	96.57	98.57		0.1242	0.0627	0.3627	82.57	94.88	97.73
Kitchen	0.1482	0.0791	0.3374	82.31	95.42	98.32		0.1819	0.0978	0.3521	78.86	93.05	96.63
Playroom	<u>0.0702</u>	<u>0.0276</u>	<u>0.2466</u>	<u>94.54</u>	98.25	99.79		0.1010	0.0476	0.3042	<u>92.11</u>	97.23	99.15
Living room	0.1033	0.0502	0.3448	89.07	97.88	99.52		0.1132	0.0568	0.3601	87.35	97.31	99.34
Bathroom	0.1456	0.0772	0.2788	83.45	96.07	98.13		0.1439	0.0570	0.2488	83.72	96.55	98.36
Standard Deviation	0.0395	0.0559	0.3384	13.36	7.50	2.79		0.0361	0.0512	0.2972	6.78	3.58	1.93
Value Max	0.2683	0.4499	1.3915	94.54	99.25	99.83		0.2125	0.3119	1.1396	92.11	99.14	99.86
Value Min	0.0702	0.0276	0.2466	54.93	83.89	93.91		0.0912	0.0372	0.2488	67.71	88.59	95.40
Easy/ Hard Summary		MIM						PixelFormer					
Easy type		playroom, private room, classroom						playroom, private room, classroom					
Hard type		large room, lounge, library						large room, lounge, library, hallway					
† M&LS-Pre		ZoeDepth(N) Results						VPD Results					
Type Breakdown	AbsRel	SqRel	RMSE	δ_1	δ_2	δ_3		AbsRel	SqRel	RMSE	δ_1	δ_2	δ_3
Private room	0.0798	<u>0.0253</u>	0.2218	93.86	<u>99.44</u>	99.90		0.0768	0.0325	0.2428	93.76	98.70	99.60
Office	0.0978	0.0447	0.3102	90.07	97.80	99.52		0.1019	0.0548	0.3374	89.52	97.52	99.26
Hallway	0.1193	0.0741	0.5271	85.84	96.95	99.10		0.1174	0.0828	0.5233	86.66	96.40	98.72
Lounge	0.1172	0.1110	0.7033	86.61	97.02	99.11		0.1313	0.1286	0.7306	83.06	95.90	98.83
Meeting room	0.0887	0.0391	0.3379	93.55	99.05	99.79		0.0992	0.0568	0.3742	91.51	98.26	99.43
Large room	0.1565	0.1701	0.9157	77.19	94.95	99.33		0.1292	0.1460	0.7903	83.90	95.87	98.89
Classroom	<u>0.0719</u>	0.0282	0.2873	<u>95.37</u>	99.43	<u>99.91</u>		0.0744	0.0344	0.3034	94.73	<u>98.94</u>	99.72
Library	0.1163	0.0875	0.6274	87.34	96.93	98.99		0.1258	0.1311	0.6885	85.22	95.34	98.62
Kitchen	0.1256	0.0589	0.2825	87.10	96.70	98.00		0.0958	0.0538	0.2649	92.56	96.36	98.64
Playroom	0.0790	0.0300	0.2508	94.21	98.09	99.88		0.0735	0.0313	0.2574	<u>95.17</u>	98.38	99.83
Living room	0.0862	0.0390	0.3036	91.72	98.31	99.58		0.0910	0.0510	0.3490	91.45	97.59	99.25
Bathroom	0.1065	0.0358	0.1880	93.64	97.64	98.17		0.0955	0.0472	0.2279	92.95	<u>97.04</u>	<u>97.98</u>
Standard Deviation	0.0250	0.0465	0.2448	6.57	1.83	0.85		0.0211	0.0444	0.1947	4.83	1.57	1.00
Value Max	0.1565	0.1701	0.9157	95.37	99.44	99.91		0.1313	0.1460	0.7903	95.17	98.94	99.83
Value Min	0.0719	0.0253	0.1880	77.19	94.95	98.00		0.0735	0.0313	0.2279	83.06	95.34	97.98
Easy/ Hard Summary		ZoeDepth(N)						VPD					
Easy type		bathroom, private room, playroom, classroom						bathroom, private room, kitchen, classroom					
Hard type		large room, lounge, library, hallway						large room, lounge, library, hallway					
† M&LS-Pre		DepthAnything Results						Unidepth Results					
Type Breakdown	AbsRel	SqRel	RMSE	δ_1	δ_2	δ_3		AbsRel	SqRel	RMSE	δ_1	δ_2	δ_3
Private room	0.0836	0.0297	0.2500	91.87	98.78	99.80		0.0609	0.0163	0.1805	<u>96.94</u>	99.50	99.89
Office	0.0990	0.0454	0.3130	88.12	97.61	99.45		0.0788	0.0322	0.2608	93.25	98.44	99.64
Hallway	0.1074	0.0683	0.4726	87.02	96.55	99.05		0.0871	0.0566	0.4608	90.83	97.14	99.10
Lounge	0.1053	0.0920	0.6310	88.34	97.69	99.33		0.0860	0.0663	0.5312	93.24	98.39	99.41
Meeting room	0.0899	0.0462	0.3591	90.28	98.52	99.76		0.0764	0.0330	0.2992	94.66	99.12	99.79
Large room	0.1051	0.0974	0.6860	88.61	97.91	99.27		0.0871	0.0688	0.5370	94.10	98.46	99.26
Classroom	0.0870	0.0426	0.3465	90.24	98.61	99.81		0.0601	0.0233	0.2589	96.67	99.52	99.93
Library	0.0947	0.0641	0.5150	90.08	98.09	99.43		0.0800	0.0498	0.4505	93.63	98.37	99.40
Kitchen	0.0863	0.0390	0.2480	91.97	99.99	99.13		0.0662	0.0235	0.2027	95.42	98.80	99.34
Playroom	0.0871	0.0416	0.3453	91.23	98.38	99.62		0.0544	0.0182	0.1983	95.60	99.30	99.89
Living room	0.0921	0.0472	0.3448	90.26	97.80	99.47		0.0670	0.0312	0.2758	94.87	98.54	99.58
Bathroom	0.0860	0.0337	0.1965	92.71	<u>98.72</u>	98.76		0.0765	0.0252	0.1600	96.40	98.00	98.52
Standard Deviation	0.0085	0.0257	0.1470	1.56	0.87	0.36		0.0118	0.0204	0.1471	1.96	0.72	0.58
Value Max	0.1074	0.0974	0.6860	92.71	99.72	99.80		0.0871	0.0688	0.5370	96.94	99.52	99.93
Value Min	0.0836	0.0297	0.1965	87.02	96.55	98.76		0.0544	0.0163	0.1600	90.83	97.14	98.52
Easy/ Hard Summary		DepthAnything						Unidepth					
Easy type		bathroom, private room, kitchen						bathroom, private room, kitchen, classroom, playroom					
Hard type		large room, lounge, library, meeting room						hallway, lounge, library, office					

even slightly outperforms fine-tuned DepthAnything. One can observe that Unidepth has larger performance gaps to others on the benchmark where all the methods are evaluated by zero-shot performance.

Discussion on robustness. Even an early method, DPT, which is also pretrained on multiple datasets and fine-tuned on NYUv2, can slightly outperform several later methods in terms of AbsRel, such as PixelFormer, IronDepth, or Decomposition, which actually won over DPT on the NYUv2 benchmark. Fig. 3 shows a visual comparison using oriental-style rooms.

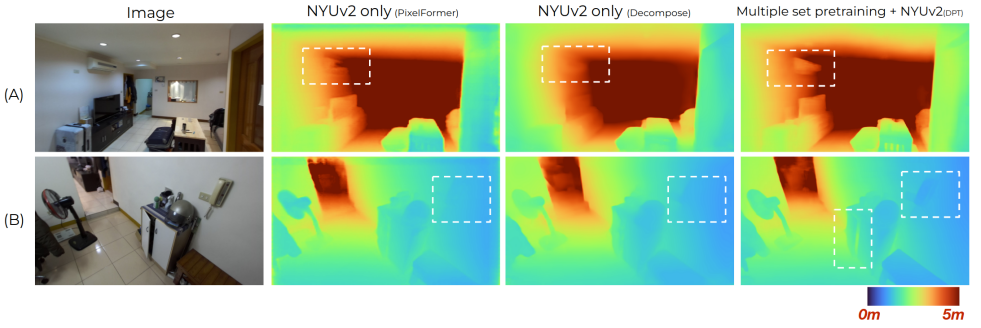


Figure 3: Zero-shot comparison between training strategies. The rooms are in oriental styles where the wall-hanging phone and air-conditioner are mostly exclusive to the cultural style. Compared with training on NYUv2 only, the multiple dataset pretraining shows higher robustness to unseen spaces, even though DPT is inferior to PixelFormer and Decompose on the standard NYUv2 dataset. Zero-shot evaluation on InSpaceType helps figure out advantages that cannot be shown if focusing on the single benchmark.

The type did not appear in NYUv2 or DPT’s training sets. Compared with single-dataset training such as PixelFormer and Decompose, DPT generalizes better to unseen spaces. The advantage in robustness cannot be shown if fixating on a single benchmark.

[II: Breakdowns by space types] Compared with overall performance that follows natural distribution, the aim here is to leave out the effect of number of samples in a type and break down performance by types to discover performance variances. Our tool shows error and accuracy metrics for each node in our hierarchical graph. See examples in the supplementary. Level-0: overall performance; Level-1: household, workspace, campus, and functional space; Level-2: private room, office, hallway, lounge, meeting room, large room, classroom, library, kitchen, playroom, living room, and bathroom; Level-3 contains more detailed types from level-2 if dividable. There are 26 leaf nodes in total. We focus on the 12 types in level-2 in the main paper and include the full type reports in the supplementary for reference. *N-only* contains the top methods, MIM and PixelFormer, among those trained on RGBD data only from NYUv2; *M&LS-Pre* contains the top methods, VPD, ZoeDepth, DepthAnything, and Unidepth, among those trained on multiple depth datasets or learned from large-scale pretraining.

Performance variance analysis. Table 2 shows performance on each space type. For N-only, though MIM is among the leading methods in Table 1 overall results and outperforms PixelFormer, its standard deviation and difference between max and min are much larger than PixelFormer, indicating a high imbalance. The gap between the best and worst (RMSE and δ_1) is prominent, which goes by (0.2466, 94.54) and (1.3915, 54.93). For M&LS-Pre in the second block, similarly, ZoeDepth has better overall performance than VPD in Table 1 but has larger performance variances shown by the standard deviation. Likewise, comparing DepthAnything and Unidepth, though DepthAnything has lower overall performance, its performance variances are slightly lower than Unidepth in terms of standard deviation for RMSE and δ_1 , showing lower imbalance.

Easy/Hard types. We also enumerate easy and hard types for each method based on the concordance in top-5 lowest error/ highest accuracy (easy) and the opposite (hard). The easy and hard types are mostly consistent, showing the natural space type distribution underlying training data. The trained models then follow the distribution and favor the head types, such

as private room and bathroom, and against the tailed types, such as library and large room. All the methods more or less have clear easy and hard types indicating bias, and some even have obvious gaps between head and tailed types from the numerical results. The lists used as references reveal where the models excel and provide guidance on their proper usage. One may expect degraded performance on the tailed types and need to curate a dataset to fine-tune to make up the gaps. Note that **we do not claim clear easy and hard types are always detrimental**, as some applications may require focusing on specific types. *We argue one needs to attend to a pretrained model’s underlying bias, understand its advantages and weakness, and be careful about overall performance reported on a single benchmark where robustness may not be fully validated.*

[III: More training sets and discussion on synthetic data curation] Going beyond the NYUv2 benchmark, there are several recent larger monocular indoor depth datasets for training purposes. We investigate the datasets by using models pretrained on them to zero-shot evaluate on InSpaceType. We study SimSIN and UniSIN [46]; the former is synthetic, and the latter is real. They are both introduced by DistDepth [46] with a focus on self-supervised learning. We adopt DistDepth’s released models for evaluation. We also study Hypersim [48], which is purely synthetic and rendered from crafted 3D CAD indoor environments, and we use its pretrained ConvNext-Base model [48]. Table 3 shows the performance and type breakdowns. Due to the synthetic-to-real and self-supervised learning challenges, their overall performance is lower than training on NYUv2 in Table 4.

Dataset characteristics and analysis. SimSIN: The dataset was built by rendering from an agent-navigating simulator [40] with scanned but incomplete household meshes from the datasets [9, 63, 42]. Thus, it may favor household spaces and bias against other types, such as workspace or campus scenes; UniSIN: It contains diverse real scenes covering workspace, household, and campus spaces and thus shows fewer hard types; Hypersim: It renders diverse indoor 3D CAD spaces with fine textures. However, many rendered scenes are highly under-/over-exposed, and many frames focus on small objects or ceilings that cut off cues for depth hints. Hypersim also contains household spaces as the majority and further includes several open or unbounded spaces.

Both SimSIN and Hypersim are synthetic, and their data curation focuses more on head types, especially private room and living room as the most common application contexts. Training on the datasets may underrepresent certain tailed types such as library, lounge, or hallway. It is worth to mention hallway is a common but easily overlooked type in synthetic datasets, especially for those who render every 3D CAD space separately without considering space connection, such as Hypersim, which shows low δ_1 compared to real scanned UniSIN.

Scene complexity for synthetic v.s. real data. One can find kitchen is a special type in SimSIN and Hypersim, which is of lower RMSE but also very low accuracy δ_1 / high AbsRel compared with other types. Kitchens are small-range with naturally lower RMSE if a network predicts near ranges. However, the lower δ_1 and higher AbsRel indicate detailed surface depth for objects is not accurately predicted. This is because kitchen scenes often abound with cluttered and small objects spread across the view (Fig. 4). Strategies of synthetic data curation, such as rendering from scanned but incomplete meshes (SimSIN²) or from crafted 3D CAD indoor environments (Hypersim³), cannot faithfully reflect the high complexity of cluttered and small objects in real scenes. The study highlights common deficiencies in synthetic data curation for synthetic-to-real transfer. One needs to consider scene complexity

²small or thin objects are usually skewed in shape or incomplete due to limited laser scan resolutions.

³most 3D CAD models favor neat and organized spaces, and crafting cluttered/ small objects takes manual efforts.



Figure 4: Real kitchen scenes contain many small objects in large areas. However, the synthetic data cannot match the complexity hindering synthetic-to-real performance.

Table 3: **Space type breakdowns and characteristics** for more real and synthetic datasets.

Dataset Study	SimSIN			UniSIN			Hypersim		
Type Breakdown	AbsRel	RMSE	δ_i	AbsRel	RMSE	δ_i	AbsRel	RMSE	δ_i
Private room	0.1509	0.4447	79.36	0.1736	0.4527	72.89	0.1321	0.3376	84.55
Office	0.1812	0.5789	74.01	0.1650	0.5016	77.12	0.1678	0.4916	76.01
Hallway	0.1597	0.6324	78.12	0.1258	0.4970	85.13	0.2126	0.8347	65.67
Lounge	0.1841	0.9037	73.86	0.1375	0.7347	83.08	0.1937	0.9403	71.31
Meeting room	0.1962	0.9417	66.91	0.1295	0.5938	84.17	0.1315	0.5333	81.49
Large room	0.1842	1.0727	72.79	0.1607	0.9449	75.36	0.2525	1.3897	56.48
Classroom	0.2069	1.0292	67.11	0.1301	0.6072	85.01	0.1258	0.4700	85.07
Library	0.1857	0.8307	75.14	0.1218	0.6921	85.88	0.1766	0.8654	73.53
Kitchen	0.2524	0.5649	59.22	0.2122	0.4950	75.66	0.2417	0.4347	62.81
Playroom	0.1597	0.5946	75.59	0.1475	0.4710	78.99	0.1629	0.5663	77.09
Living room	0.1600	0.5284	77.05	0.1642	0.5108	76.51	0.1485	0.4519	80.91
Bathroom	0.1751	0.3900	74.22	0.1381	0.2163	84.89	0.1648	0.2908	76.11
All	0.1746	0.6877	74.72	0.1426	0.5414	80.23	0.1592	0.5803	77.95
Summary	SimSIN			UniSIN			Hypersim		
Easy type	living room, private room			bathroom, hallway			private room, living room, classroom		
Hard type	large room, classroom, meeting room, lounge			large room			large room, library, hallway, lounge		

Table 4: **Cross-group generalization.** The header \rightarrow specifies a source training group, and the rows below show testing groups and results.

Test group	G1 \rightarrow			G2 \rightarrow			G3 \rightarrow		
	AbsRel	RMSE	δ_i	AbsRel	RMSE	δ_i	AbsRel	RMSE	δ_i
G1	0.0735	0.1851	95.42	0.1415	0.3478	82.44	0.1886	0.4744	73.01
G2	0.1588	0.5488	79.10	0.0790	0.2470	94.79	0.1945	0.6101	72.88
G3	0.2644	1.1552	62.05	0.2107	0.9400	70.18	0.0729	0.3470	95.65

while creating synthetic data to achieve better in real scenes.

[IV: Dataset ablation for generalization study] Aside from the above cross-dataset generalization experiments, consider a case when a space type is missed in a dataset, how hard is it, and what are key factors to generalize to unseen types? The study uses all the collected InSpaceType data to form a split with about 40K RGBD pairs, where the previous 1260 evaluation pairs and their nearby 2 frames are excluded. This 40K split is divided into 3 groups by similarity in functions. G1 (household space): private room, kitchen, living room, and bathroom; G2 (workspace and campus): office, hallway, meeting room, and classroom; G3 (large functional space): lounge, large room, playroom, and library. Then we train models⁴ on each group and evaluate on the 1260-pair evaluation set. For instance, G1 \rightarrow G2 means training on G1, where a model only has seen G1’s type, and testing on data of G2’s types in the evaluation set. Table 4 provides the results.

Generalization to unseen types (e.g., G1 \rightarrow G3) is more challenging than seen types (e.g., G1 \rightarrow G1). One can observe that household space (G1) and workspace (G2) are easier to

⁴without loss of generality, we use general-purpose ConvNeXt-L and standard L_2 , smoothness, and SILog loss. We train by 30 epochs, which is adequate for convergence regarding loss. The learning rate is set at 0.0001, momentum at (0.9, 0.999), and weight decay at 0.01 with an AdamW optimizer.

generalize to each other than generalize to large functional space (G3), and vice versa for $G3 \rightarrow G1/G2$. G1 and G2 are mainly distinct in object arrangements and appearance, whereas G1 and G3 mainly differ in depth ranges. The average maximal depth is 3.78m for G1, 5.49m for G2, and 12.08m for G3. The results indicate the scene scale is the key factor. Training on one group inherently introduces a bias towards the output depth ranges. When presented with a scene in a much different range, the model struggles to accurately estimate the corresponding depth range.

5 Conclusion

The work pioneers studying space types in indoor monocular depth for practical purposes, especially with the advent of many large models, but the evaluation and quality assessment still primarily focus on a single and older benchmark. First, we present novel InSpaceType Dataset that meets the high-resolution and high-quality RGBD data requirements for cutting-edge applications in AR/VR displays and indoor robotics. Previous works focusing on methods may overlook performance variances. We use InSpaceType to study 13 recent high-performing methods and analyze their zero-shot cross-dataset performance for both overall results and performance variances across space types. Even some top methods have severe imbalance, and some methods are actually less imbalanced than higher-performing ones.

We extend our analysis to more synthetic and real datasets, including SimSIN, UniSIN, and Hypersim, to reveal their bias and guide proper usage. Especially, current synthetic data curation may not faithfully reflect the real-world high complexity in cluttered and small objects, and we suggest the best practice. Further, they may miss some common types like hallway if rendering single 3D CAD spaces separately. We further do ablation on InSpaceType and find space scale is the key factor that hinders generalization. As part of our contribution, our released tools for both research and practical aids, including codes and datasets, can diagnose a pretrained model and show its hierarchical performance breakdown. Overall, this work underscores the importance of considering performance variances in the practical deployment of models, a crucial aspect often overlooked in the field.

References

- [1] Hardware.cast technical publications series. <https://gmvc.cast.uark.edu/scanning/hardware/microsoft-kinect-resourceshardware>.
- [2] Ashutosh Agarwal and Chetan Arora. Attention attention everywhere: Monocular depth prediction with skip attention. In *WACV*, 2023.
- [3] Gwangbin Bae, Ignas Budvytis, and Roberto Cipolla. Irondepth: Iterative refinement of single-view depth using surface normal and its uncertainty. *BMVC*, 2022.
- [4] Hangbo Bao, Li Dong, Songhao Piao, and Furu Wei. Beit: Bert pre-training of image transformers. *ICLR*, 2021.
- [5] Shariq Farooq Bhat, Ibraheem Alhashim, and Peter Wonka. Adabins: Depth estimation using adaptive bins. In *CVPR*, 2021.
- [6] Shariq Farooq Bhat, Ibraheem Alhashim, and Peter Wonka. Localbins: Improving depth estimation by learning local distributions. In *ECCV*, 2022.

- [7] Shariq Farooq Bhat, Reiner Birkel, Diana Wofk, Peter Wonka, and Matthias Müller. Zoedepth: Zero-shot transfer by combining relative and metric depth. *arXiv preprint arXiv:2302.12288*, 2023.
- [8] Jia-Wang Bian, Huangying Zhan, Naiyan Wang, Tat-Jun Chin, Chunhua Shen, and Ian Reid. Auto-rectify network for unsupervised indoor depth estimation. *TPAMI*, 2021.
- [9] Angel Chang, Angela Dai, Thomas Funkhouser, Maciej Halber, Matthias Niebner, Manolis Savva, Shuran Song, Andy Zeng, and Yinda Zhang. Matterport3D: Learning from RGB-D data in indoor environments. In *3DV*, 2017.
- [10] Kangle Deng, Andrew Liu, Jun-Yan Zhu, and Deva Ramanan. Depth-supervised nerf: Fewer views and faster training for free. In *CVPR*, 2022.
- [11] Catherine Diaz, Michael Walker, Danielle Albers Szafr, and Daniel Szafr. Designing for depth perceptions in augmented reality. In *2017 IEEE international symposium on mixed and augmented reality (ISMAR)*, 2017.
- [12] Alexey Dosovitskiy, Lucas Beyer, Alexander Kolesnikov, Dirk Weissenborn, Xiaohua Zhai, Thomas Unterthiner, Mostafa Dehghani, Matthias Minderer, Georg Heigold, Sylvain Gelly, et al. An image is worth 16x16 words: Transformers for image recognition at scale. In *ICLR*, 2020.
- [13] Fabrizio Flacco, Torsten Kröger, Alessandro De Luca, and Oussama Khatib. A depth space approach to human-robot collision avoidance. In *ICRA*, 2012.
- [14] Huan Fu, Mingming Gong, Chaohui Wang, Kayhan Batmanghelich, and Dacheng Tao. Deep ordinal regression network for monocular depth estimation. In *CVPR*, 2018.
- [15] Hualie Jiang, Laiyan Ding, Junjie Hu, and Rui Huang. Plnet: Plane and line priors for unsupervised indoor depth estimation. In *3DV*, 2021.
- [16] Jinyoung Jun, Jae-Han Lee, Chul Lee, and Chang-Su Kim. Depth map decomposition for monocular depth estimation. In *ECCV*, 2022.
- [17] Doyeon Kim, Woonghyun Ga, Pyungwhan Ahn, Donggyu Joo, Sehwan Chun, and Junmo Kim. Global-local path networks for monocular depth estimation with vertical cutdepth. *arXiv:2201.07436*, 2022.
- [18] Tobias Koch, Lukas Liebel, Friedrich Fraundorfer, and Marco Korner. Evaluation of cnn-based single-image depth estimation methods. In *ECCVW*, 2018.
- [19] Jin Han Lee, Myung-Kyu Han, Dong Wook Ko, and Il Hong Suh. From big to small: Multi-scale local planar guidance for monocular depth estimation. *arXiv preprint arXiv:1907.10326*, 2019.
- [20] Junwoo Lee and Bummo Ahn. Real-time human action recognition with a low-cost rgb camera and mobile robot platform. *Sensors*, 2020.
- [21] Boying Li, Yuan Huang, Zeyu Liu, Danping Zou, and Wenxian Yu. Structdepth: Leveraging the structural regularities for self-supervised indoor depth estimation. In *ICCV*, 2021.
- [22] Wang Li, Junfeng Wang, Maoding Liu, and Shiwen Zhao. Real-time occlusion handling for augmented reality assistance assembly systems with monocular images. *Journal of Manufacturing Systems*, 2022.
- [23] Zhenyu Li, Zehui Chen, Xianming Liu, and Junjun Jiang. Depthformer: Exploiting long-range correlation and local information for accurate monocular depth estimation. *arXiv preprint arXiv:2203.14211*, 2022.

- [24] Zhenyu Li, Xuyang Wang, Xianming Liu, and Junjun Jiang. Binsformer: Revisiting adaptive bins for monocular depth estimation. *arXiv preprint arXiv:2204.00987*, 2022.
- [25] Ce Liu, Suryansh Kumar, Shuhang Gu, Radu Timofte, and Luc Van Gool. Va-depthnet: A variational approach to single image depth prediction. In *ICLR*, 2023.
- [26] Fayao Liu, Chunhua Shen, and Guosheng Lin. Deep convolutional neural fields for depth estimation from a single image. In *CVPR*, 2015.
- [27] Ze Liu, Yutong Lin, Yue Cao, Han Hu, Yixuan Wei, Zheng Zhang, Stephen Lin, and Baining Guo. Swin transformer: Hierarchical vision transformer using shifted windows. In *ICCV*, 2021.
- [28] Zhuang Liu, Hanzi Mao, Chao-Yuan Wu, Christoph Feichtenhofer, Trevor Darrell, and Saining Xie. A convnet for the 2020s. *CVPR*, 2022.
- [29] Xuan Luo, Jia-Bin Huang, Richard Szeliski, Kevin Matzen, and Johannes Kopf. Consistent video depth estimation. *ACM Transactions on Graphics (TOG)*, 2020.
- [30] Wolfgang Mehringer, Markus Wirth, Daniel Roth, Georg Michelson, and Bjoern M Eskofier. Stereopsis only: Validation of a monocular depth cues reduced gamified virtual reality with reaction time measurement. *IEEE Transactions on Visualization and Computer Graphics*, 2022.
- [31] Jia Ning, Chen Li, Zheng Zhang, Chunyu Wang, Zigang Geng, Qi Dai, Kun He, and Han Hu. All in tokens: Unifying output space of visual tasks via soft token. In *ICCV*, 2023.
- [32] Luigi Piccinelli, Yung-Hsu Yang, Christos Sakaridis, Mattia Segu, Siyuan Li, Luc Van Gool, and Fisher Yu. Unidepth: Universal monocular metric depth estimation. In *CVPR*, 2024.
- [33] Santhosh K Ramakrishnan, Aaron Gokaslan, Erik Wijmans, Oleksandr Maksymets, Alex Clegg, John Turner, Eric Undersander, Wojciech Galuba, Andrew Westbury, Angel X Chang, et al. Habitat-matterport 3D dataset (HM3D): 1000 large-scale 3D environments for embodied AI. *NeurIPS Datasets and Benchmarks Track*, 2021.
- [34] Michael Ramamonjisoa, Michael Firman, Jamie Watson, Vincent Lepetit, and Daniyar Turmukhambetov. Single image depth prediction with wavelet decomposition. In *CVPR*, 2021.
- [35] René Ranftl, Katrin Lasinger, David Hafner, Konrad Schindler, and Vladlen Koltun. Towards robust monocular depth estimation: Mixing datasets for zero-shot cross-dataset transfer. *TPAMI*, 2020.
- [36] René Ranftl, Alexey Bochkovskiy, and Vladlen Koltun. Vision transformers for dense prediction. *ICCV*, 2021.
- [37] Elisa Ricci, Wanli Ouyang, Xiaogang Wang, Nicu Sebe, et al. Monocular depth estimation using multi-scale continuous crfs as sequential deep networks. *TPAMI*, 2018.
- [38] Mike Roberts, Jason Ramapuram, Anurag Ranjan, Atulit Kumar, Miguel Angel Bautista, Nathan Paczan, Russ Webb, and Joshua M Susskind. Hypersim: A photorealistic synthetic dataset for holistic indoor scene understanding. In *ICCV*, 2021.
- [39] Robin Rombach, Andreas Blattmann, Dominik Lorenz, Patrick Esser, and Björn Ommer. High-resolution image synthesis with latent diffusion models. In *CVPR*, 2022.
- [40] Manolis Savva, Abhishek Kadian, Oleksandr Maksymets, Yili Zhao, Erik Wijmans, Bhavana Jain, Julian Straub, Jia Liu, Vladlen Koltun, Jitendra Malik, et al. Habitat: A platform for embodied ai research. In *CVPR*, 2019.

- [41] Nathan Silberman, Derek Hoiem, Pushmeet Kohli, and Rob Fergus. Indoor segmentation and support inference from rgb-d images. In *ECCV*, 2012.
- [42] Julian Straub, Thomas Whelan, Lingni Ma, Yufan Chen, Erik Wijmans, Simon Green, Jakob J Engel, Raul Mur-Artal, Carl Ren, Shobhit Verma, et al. The replica dataset: A digital replica of indoor spaces. *arXiv preprint arXiv:1906.05797*, 2019.
- [43] Lei Tai, Jingwei Zhang, Ming Liu, and Wolfram Burgard. Socially compliant navigation through raw depth inputs with generative adversarial imitation learning. In *ICRA*, 2018.
- [44] Igor Vasiljevic, Nick Kolkin, Shanyi Zhang, Ruotian Luo, Haochen Wang, Falcon Z Dai, Andrea F Daniele, Mohammadreza Mostajabi, Steven Basart, Matthew R Walter, et al. Diode: A dense indoor and outdoor depth dataset. *arXiv preprint arXiv:1908.00463*, 2019.
- [45] Cho-Ying Wu, Xiaoyan Hu, Michael Happold, Qiangeng Xu, and Ulrich Neumann. Geometry-aware instance segmentation with disparity maps. *arXiv preprint arXiv:2006.07802*, 2020.
- [46] Cho-Ying Wu, Jialiang Wang, Michael Hall, Ulrich Neumann, and Shuochen Su. Toward practical monocular indoor depth estimation. In *CVPR*, 2022.
- [47] Cho-Ying Wu, Yiqi Zhong, Junying Wang, and Ulrich Neumann. Meta-optimization for higher model generalizability in single-image depth prediction. *arXiv preprint arXiv:2305.07269*, 2023.
- [48] Zhenda Xie, Zigang Geng, Jingcheng Hu, Zheng Zhang, Han Hu, and Yue Cao. Revealing the dark secrets of masked image modeling. In *CVPR*, 2023.
- [49] Lihe Yang, Bingyi Kang, Zilong Huang, Xiaogang Xu, Jiashi Feng, and Hengshuang Zhao. Depth anything: Unleashing the power of large-scale unlabeled data. In *CVPR*, 2024.
- [50] Wei Yin, Yifan Liu, Chunhua Shen, and Youliang Yan. Enforcing geometric constraints of virtual normal for depth prediction. In *ICCV*, 2019.
- [51] Wei Yin, Jianming Zhang, Oliver Wang, Simon Niklaus, Long Mai, Simon Chen, and Chunhua Shen. Learning to recover 3d scene shape from a single image. In *CVPR*, 2021.
- [52] Weihao Yuan, Xiaodong Gu, Zuozhuo Dai, Siyu Zhu, and Ping Tan. New crfs: Neural window fully-connected crfs for monocular depth estimation. *CVPR*, 2022.
- [53] Chaoqiang Zhao, Matteo Poggi, Fabio Tosi, Lei Zhou, Qiyu Sun, Yang Tang, and Stefano Mattoccia. Gasmono: Geometry-aided self-supervised monocular depth estimation for indoor scenes. In *ICCV*, 2023.
- [54] Wenliang Zhao, Yongming Rao, Zuyan Liu, Benlin Liu, Jie Zhou, and Jiwen Lu. Unleashing text-to-image diffusion models for visual perception. *ICCV*, 2023.